J Plant Growth Regul (2013) 32:353–361
DOI 10.1007/s00344-012-9305-5

Regulation of Metabolites, Gene Expression, and Antioxidant Enzymes to Environmentally Relevant Lead and Zinc in the Halophyte *Suaeda salsa*

Huifeng Wu · Xiaoli Liu · Jianmin Zhao · Junbao Yu

Received: 14 November 2011 / Accepted: 2 August 2012 / Published online: 28 November 2012

Abstract As a pioneer halophyte, *Suaeda salsa* can grow in the intertidal zones, which are often polluted by heavy metals from both terrigenous wastewater and tidewater containing high concentrations of heavy metals. Therefore *S. salsa* is potentially suitable as a biomonitor for heavy-metal pollution in the intertidal zones. In this study, regulation of metabolites, gene expression, and antioxidant status of environmentally relevant lead and zinc were characterized using NMR-based metabolomics, real-time quantitative reverse transcription polymerase chain reaction, and antioxidant enzyme activities. In Pb-exposed *S. salsa* samples, only decreased tyrosine was observed, with statistical significance approaching 0.05. Metabolic biomarkers in Zn-exposed *S. salsa* samples included increased amino acids (valine, isoleucine, leucine, threonine, asparagine, and phenylalanine), and decreased acetate, glucose, ferulate, and fumarate. Increased succinate, aspartate, and malonate and decreased fructose were uniquely found in mixed Pb- and Zn-exposed samples in addition to the similar metabolic changes such as alanine, glucose, fumarate, and ferulate in Zn-exposed samples. Based on the metabolic biomarkers, gene expressions, and antioxidant enzyme activities, both Zn and mixed Pb and Zn induced significant oxidative stress and disturbances in energy metabolism, photosynthesis/glucogenesis, and protein biodegradation in *S. salsa*. However, environmentally relevant Pb could induce slight oxidative stress in *S. salsa* as indicated by increased catalase gene expression levels and catalase activities.

Keywords Lead · Zinc · Biomarker · *Suaeda salsa* · Metabolomics · Antioxidant enzyme

H. Wu (✉) · X. Liu · J. Zhao · J. Yu
Key Laboratory of Coastal Zone Environment Processes, Shandong Provincial Key Laboratory of Coastal Zone Environment Processes, Yantai Institute of Coastal Zone Research, Chinese Academy of Sciences, Yantai 264003, People's Republic of China
e-mail: hfwu@yic.ac.cn

X. Liu
The Graduate School of Chinese Academy of Sciences, Beijing 100049, People's Republic of China

Introduction

The intertidal zone is the area that is above water at low tide and under water at high tide. This area can be easily polluted by pollutants from both terrigenous wastewater and tidewater. In the intertidal zones of the Yellow River Delta, some heavy-metal contaminants such as cadmium (Cd), mercury (Hg), lead (Pb), and zinc (Zn) have commonly been found due to the discharge of industrial wastewaters (Zhang 2001; Mao and others 2009). These heavy metals can be accumulated by different types of organisms such as shellfish, fish, and plants and can lead to hazardous health effects in the human body via the food chain (Garg and Aggarwal 2011; Sun and others 2011; Noriega and others 2012). Among these heavy-metal contaminants, lead and zinc concentrations have been up to 70 and 120 μg L^{-1} in seawater from the Bohai Sea, respectively (Zhang 2001; Mao and others 2009). Lead is a nonessential element for organisms and causes various toxicities, including neurotoxicity, nephrotoxicity, cardiovascular disease, genotoxicity, immunotoxicity, and carcinogenicity in animals (Zurich and others 2002; van Wijngaarden and Dosemeci 2006; Jain and others 2007). Zinc is essential to organisms; however, excessive Zn can induce potential toxicities such as genotoxicity and immunotoxicity in vertebrates (Hogstrand and Wood 1996).

The intertidal zones include different types of organisms such as shellfish, some species of coral, and halophytes. The halophyte *Suaeda salsa* is a pioneer plant in the intertidal zones in the Yellow River Delta (Zhao 1991). As a matter of fact, *S. salsa* has been advantageous in environmental sciences and has been used for the phytoremediation of heavy-metal pollutants or increasing salinity in the intertidal zones or saline soils (Zhu and others 2005; Li and others 2007; Xu and others 2007; Wu and others 2012). Due to its high tolerance to salinity and immobility, *S. salsa* exhibits the potential as a bioindicator for environmental monitoring of saline soil and intertidal zones with high salinity. For example, Zhu and others (2005) studied the bioavailability and distribution of heavy metals (Cu, Zn, Pb, and Cd) in *S. salsa* and suggested that *S. salsa* was applicable as a heavy-metal bioindicator and for the phytoremediation of heavy-metal-polluted soil. As a pioneer halophyte in the intertidal zones along the Bohai Sea, the physiological and molecular responses of *S. salsa* to salinity have been studied extensively and hence *S. salsa* has been suggested as a bioindicator of saline soils (Zhang and others 2001; Li and others 2002, 2004; Wang and others 2001, 2004; Han and others 2005). Previously, we reported the regulated metabolites that are characteristic of the toxicological effects induced by environmentally relevant Cd in the aboveground part of the seedlings of *S. salsa* using NMR-based metabolomics (Liu and others 2011a).

In this study, ^{1}H-NMR-based metabolomics were applied to the halophyte *S. salsa* exposed to environmentally relevant lead (20 μg L^{-1}) and zinc (100 μg L^{-1}) to detect the regulatory metabolites in the aboveground part of the plant, and then to characterize the subacute toxicological effects induced by lead and zinc in *S. salsa*. The gene expressions of key enzymes involved in osmotic regulation, antioxidation, and photosynthesis were quantified using the real-time quantitative reverse transcription polymerase chain reaction (RT-PCR) technique. Among the selected enzymes, *Myo*-inositol-1-phosphate synthase (*INPS*, BE644574) is the key enzyme in the biosynthesis of *Myo*-inositol (Ins) that plays an important role in salt tolerance in the common ice plant (Vernon and Bohnert 1992; Nelson and others 1998). In higher plants, betaine is synthesized by oxidation of choline: choline → betaine aldehyde → betaine. The two steps are catalyzed by choline monooxygenase (*CMO*, AW991015) and betaine aldehyde dehydrogenase (*BADH*, DQ641924), respectively (Greenway and Osmond 1972). Catalase (*CAT*, AW990998) and glutathione peroxidase (*GPx*, AW991114) are common antioxidant enzymes that protect cells from oxidative stresses. $NADP^{+}$-malate dehydrogenase (*MDH*, AW991100) is one of the key enzymes in photosynthesis and catalyzes malate synthesis from oxaloacetate (Hoshino and others 1978). In addition, the antioxidant enzymatic activities were measured to examine the antioxidant status in the aboveground part of *S. salsa* exposed to heavy metals. Based on the regulated metabolites, genes, and antioxidant enzymes, we expected to illustrate the toxicological effects of two typical heavy-metal contaminants, lead and zinc, in the halophyte *S. salsa* in the intertidal zones of the Yellow River Delta.

Materials and Methods

Chemicals

Sodium dihydrogen phosphate (Na_2HPO_4), disodium hydrogen phosphate (NaH_2PO_4), mercury chloride ($HgCl_2$), lead nitrate ($Pb(NO_3)_2$), and zinc chloride ($ZnCl_2$) (all analytical grade), and metabolite extraction solvents, including methanol and chloroform, were purchased from Guoyao Chemical Co. Ltd. (Shanghai, China). Deuterium oxide (D_2O, 99.9 % in D) and sodium 3-trimethylsilyl[2,2,3,3-D4]propionate (TSP) were purchased from Cambridge Isotope Laboratories (Miami, FL, USA). The antioxidant enzyme kits were purchased from Nanjing Jiancheng Bioengineering Institute (Nanjing, China).

Cultivation of *S. salsa* Under Heavy-Metal Exposure

The seeds of *S. salsa* were collected from the Yellow River Delta in November 2010 and stored in a refrigerator at 4 °C for 7 months. The seeds were surface sterilized using 0.5 % $HgCl_2$ for 10 min and then washed in sterilized double-distilled water three times. Forty seeds of similar size were sown in sand in four replicate 20 cm-diameter plastic jugs ($n = 10$ per jug; one control and three heavy-metal-exposed groups). The sand was collected from the intertidal zones of the Yellow River Delta and rinsed in diluted nitric acid (1 %) to eliminate impurities such as organic matter and metal ions. The sown *S. salsa* seeds were irrigated with Hoagland's nutrient solution. After 15 days, all the seedlings of the exposed groups were irrigated with the Hoagland's nutrient solution containing 20 μg L^{-1} lead (as $Pb(NO_3)_2$), 100 μg L^{-1} zinc (as $ZnCl_2$), and the mixed 20 μg L^{-1} lead and 100 μg L^{-1} zinc, respectively. The concentrations of heavy metals were environmentally equivalent to the real situation of pollution in the Yellow River Delta (Zhou and Yan 1997; Zhang 2001). The culture condition was temperature of 28 ± 4 °C, photoperiod of 12 h light/12 h darkness, relative humidity of 70 %, and photosynthetically active radiation of 600 μmol m^{-2} s^{-1}. After exposure for 15 days, the *S. salsa* seedlings ($n = 10$) from the control and heavy-metal-exposed groups were randomly harvested. After a quick measure of the total length and weight of

seedlings, all the aboveground parts were flash-frozen in liquid nitrogen and stored at −80 °C prior to metabolite and total RNA extraction, enzymatic assay, and metal determination.

Metabolite Extraction

Polar metabolites were extracted from the aboveground part of *S. salsa* ($n = 6$) using the solvent system of methanol/water (1/1) as described previously (Kim and Verpoorte 2010; Liu and others 2011a, b). Briefly, the aboveground part of the seedling was ground in a liquid N_2-cooled mortar and pestle. The tissue powder (weighing from 250 to 300 mg per sample) was transferred to a tube containing approximately 50 ceramic beads that were 1 mm in diameter, and then thoroughly homogenized in 3.33 mL g^{-1} methanol/water (1/1) using a high throughput homogenizer (Precellys 24, Bertin, France). After homogenization, the sample was transferred to an Eppendorf tube and vortexed three times. Following centrifugation (3,000×*g*, 10 min, 4 °C), the supernatant was removed and then lyophilized. It was subsequently resuspended in 600 µL of 100 mM phosphate buffer (Na_2HPO_4 and NaH_2PO_4, including 0.5 mM TSP, pH 7.0) in D_2O. The mixture was vortexed and then centrifuged at 3,000×*g* for 5 min at 4 °C. The supernatant substance (550 µL) was pipetted into a 5 mm NMR tube prior to NMR analysis.

NMR Spectroscopy

Extracts of *S. salsa* samples were analyzed on a Bruker AV 500 NMR spectrometer at 500.18 MHz (298 K), as described previously (Liu and others 2011a, b). One-dimensional (1D) ^{1}H-NMR spectra were obtained using 11.9 µs pulse, 6,009.6 Hz spectral width, 0.1 s mixing time, and 3.0 s relaxation delay with standard 1D NOESY pulse sequence, with 128 transients collected into 16,384 data points. Data sets were zero-filled to 32,768 points, and exponential line broadening of 0.3 Hz was applied before Fourier transformation. All ^{1}H-NMR spectra were phased, baseline-corrected, and calibrated (TSP at 0.0 ppm) manually using TopSpin (version 2.1, Bruker). NMR spectral peaks were assigned following tabulated chemical shifts (Fan 1996) and using Chenomx software (evaluation version, Chenomx Inc., Canada).

Spectral Preprocessing and Multivariate Data Analysis

One-dimensional ^{1}H-NMR spectra were converted to a format for multivariate analysis using custom-written ProMetab software in Matlab (version 7.0; The MathsWorks, Natick, MA, USA). Each spectrum was divided into 0.01 ppm bins between 0.2 and 10.0 ppm, with bins from 4.70 to 5.20 ppm (water) excluded from all the NMR spectra. Bins between 8.32 and 8.35 ppm, between 8.26 and 8.28 ppm, between 8.24 and 8.26 ppm, between 8.18 and 8.20 ppm, between 7.97 and 8.01 ppm, between 7.70 and 7.85 ppm, between 7.52 and 7.56 ppm, and between 6.53 and 6.58 ppm containing pH-sensitive NMR peaks were compressed into single bins. The total spectral area of the remaining bins was normalized to unity to facilitate the comparison between the spectra. All the NMR spectra were generalized log-transformed with a transformation parameter $\lambda = 5.0 \times 10^{-8}$, which was optimized using ProMetab software to stabilize the variance across the spectral bins and to increase the weightings of the less intense peaks (Parsons and others 2007). Data were mean-centered before principal components analysis (PCA) using PLS Toolbox (version 4.0, Eigenvector Research, Manson, WA, USA).

PCA is an exploratory unsupervised pattern recognition method of analysis that is blind to the identity of each sample and serves to reduce the dimensionality of data and summarize the similarities and differences between multiple NMR spectra (Keun and others 2003; Xu 2004). The principal component score plots were used to visualize general clusters between various groups of samples. One way analysis of variance (ANOVA) was conducted on PC scores from each group to test statistical significance ($p < 0.05$) of separations. Chenomx software (evaluation version) was then employed to identify and quantify potentially significant metabolites between various groups (Hines and others 2007). Metabolite concentrations were normalized to the mass of *S. salsa* tissue by calculating the concentration of metabolites in each NMR tube. A *p* value of 0.05 was considered significant for the ANOVA on the metabolites between control and exposed groups.

Total RNA Extraction and Gene Quantification

Total RNA from the aboveground part of the *S. salsa* seedlings of ($n = 6$ for each group) was isolated following the manufacturer's directions (Invitrogen, Carlsbad, CA, USA). Gene-specific primers for *myo*-inositol 1-phosphate synthase (*INPS*), choline monooxygenase (*CMO*), betaine aldehyde dehydrogenase (*BADH*), catalase (*CAT*), glutathione peroxidase (*GPx*), and the internal control *actin* were used to amplify amplicons specific for *S. salsa*. The sequences of primers and the length of the amplicons are given in Table 1. In a 96-well plate, each sample was run in triplicate in a total volume of 20 µL containing 10 µL of 2× SYBR® Premix Ex Taq™ (TaKaRa, Shiga, Japan), 0.4 µL of 50× ROX Reference DYE II, 4.8 µL of DEPC-treated H_2O, 0.4 µL of each primer, and 4.0 µL of 1:20 diluted cDNA. The fluorescent real-time quantitative PCR program was as follows: 50 °C for 2 min and 95 °C for 10 min, followed by 40 cycles of 94 °C for 15 s, 58 °C for

Table 1 GenBank accession numbers, primers, and amplicons of cDNA sequences from *S. salsa*

Gene	GenBank accession no.	Forward primer (5′–3′)	Reverse primer (5′–3′)	Length of the amplicon (bp)
INPS	BE644574	TAGTTCACGAGAATCGCAAAG	CCAAGTTTGGGAACATGAGT	100
CMO	AW991015	TTTCCCTGCTTCTTCAACCAC	TCATGAGAGTAGAAGGCAGGT	147
BADH	DQ641924	GAGTTGGCATCTGTGACTTG	ACCCGCATCTGGACCTAATC	105
CAT	AW990998	ACTGAAAATGAGCAACTGGC	GGTATCAGCATAGGCGAAAG	105
GPx	AW991114	GTCTCTCACATCTCTCTGCTCTCCT	GCAACATTGACAACAAGGAGGAC	272
MDH	AW991100	TGAGGGAAGTTAGCATTGGCAT	TTGAGTGCTTTTCCTTGCTCAGC	157
Actin	BE231408	GCCCTGGACTTCGAACAA	CGTTGCCAATGGTGATGA	195

45 s, and 72 °C for 30 s. Dissociation curve analysis of amplification products was performed at the end of each PCR to confirm that only one PCR product was amplified and detected. After the PCR program, data were analyzed with the ABI 7500 SDS software (Applied Biosystems, Foster City, CA, USA). To maintain consistency, the baseline was set automatically by the software. The comparative CT method ($2^{-\Delta\Delta CT}$ method) was used to analyze the expression level of the genes (Livak and Schmittgen 2001). The results of gene expressions were subjected to *t* test analysis, and statistical significance was defined as $p < 0.05$.

Measurement of Antioxidant Enzyme Activities

The aboveground part of the *S. salsa* seedlings ($n = 6$) was ground in liquid nitrogen, and antioxidant enzyme activities were assayed by a multiscan spectrum microplate spectrophotometer (Infinite M200, TECAN) according to the manufacturer's protocols using enzyme kits (Jiancheng, Nanjing, China). In this work, the antioxidant enzymes for measuring activity included superoxide dismutase (SOD, EC 1.15.1.1), peroxidase (POD, EC 1.11.1.7), glutathione *S*-transferase (GST, EC 2.5.1.18) catalase (CAT, EC 1.11.1.6), and glutathione peroxidase (GPx, EC 1.11.1.9). Protein concentration was determined by the Coomassie brilliant blue G-250 dye-binding method, with bovine serum albumin as a standard (Bradford 1976). All the enzyme activities were expressed as U mg^{-1} protein.

Heavy-Metal Concentrations in Plant Tissues

The remaining samples of the aboveground parts of *S. salsa* ($n = 4$) were dried at 80 °C to a constant weight. The dried tissue was accurately weighed and digested in concentrated nitric acid (70 %, Fisher Scientific, Waltham, MA, USA) using a microwave digestion system (CEM, MAR5). After digestion, all samples were diluted appropriately with ultrapure water for the quantification of Pb and Zn using ICP-MS (Agilent 7500i, Agilent Technologies, Santa Clara, CA, USA). GBW07605 tea leaves (State Bureau of Technical Supervision, P. R. China) were employed as certified reference materials for metal analysis to ensure internal quality assurance/quality control (QA/QC) practices (Li and others 2012). The spike recovery of target elements, as tested by three individual spiking experiments, was restricted within 93.5–104.7 % for Pb and 95.4–106.5 % for Zn at the level of 5 ng g^{-1}. The concentrations of Pb and Zn in the certified standards were determined to be 4.2 ± 0.4 μg g^{-1} for Pb (certified value $= 4.4 \pm 0.3$ μg g^{-1}) and 25.6 ± 2.8 μg g^{-1} for Zn (certified value $= 26.3 \pm 2.0$ μg g^{-1}).

Statistical Analysis

Data of growth parameters and enzyme activities were expressed as mean ± SD ($n = 6$). The data were statistically analyzed using the Statistics toolbox in Matlab (version 7.0; The MathsWorks, Natick, MA, USA). One-way ANOVA (analysis of variance) with Tukey's test was conducted on the data, and significant difference was defined at $p < 0.05$.

Results

Plant Growth

Table 2 gives the weight and length of the *S. salsa* seedlings exposed to Pb, Zn, and combined Pb and Zn (designated as Pb + Zn) for 15 days. Plant growth was significantly (ANOVA, $p < 0.05$) inhibited by Pb and Pb + Zn exposure in terms of decreased weight or length. The average weight of *S. salsa* seedlings from the Zn-exposed group was lower than that of the control group, with a statistical significance approaching 0.05. Obviously, all the heavy-metal exposures inhibited plant growth after exposure for 15 days.

Antioxidant Enzyme Activities

After exposure to Zn and Pb + Zn, the average activities of the antioxidant enzymes, including SOD, GPx, and CAT,

Table 2 The growth (weight of aboveground parts and length of whole seedling) of *S. salsa* after Pb (20 μg L^{-1}), Zn (100 μg L^{-1}), and combined Pb (20 μg L^{-1}) and Zn (100 μg L^{-1}) exposures for 15 days

Treatment	Control	Pb	Zn	Pb + Zn
Weight (g)	5.29 ± 1.54	3.89 ± 0.34*	3.99 ± 0.84#	4.00 ± 1.36#
Length (cm)	28.35 ± 2.30	27.20 ± 1.70	27.60 ± 1.79	25.74 ± 1.08*

Significant difference (* $p < 0.05$) among groups was tested by one-way analysis of variance

Statistical significance between control and exposed groups approached 0.05 ($p < 0.1$)

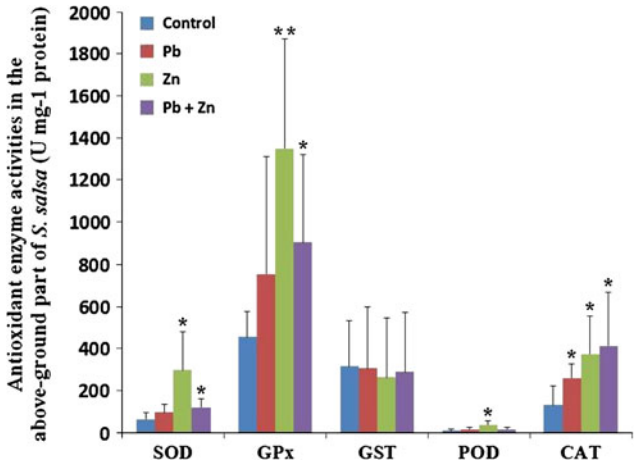

Fig. 1 The antioxidant enzyme activities (U mg^{-1} protein) of *SOD*, *GST*, *POD*, *CAT*, and *GPx* in the aboveground parts of seedlings from control and heavy-metal-exposed *S. salsa* groups

were significantly ($p < 0.05$) increased in the aboveground parts of the seedlings (Fig. 1). The significantly ($p < 0.05$) elevated activities of POD were observed only in Zn-exposed *S. salsa* samples. In Pb-exposed *S. salsa* samples, only CAT activities were significantly ($p < 0.05$) upregulated. However, there were no significant alterations to GST activities in any heavy-metal-exposed *S. salsa* groups.

Metal Accumulation

Table 3 gives the accumulated metal concentrations in the aboveground tissues of *S. salsa* after exposure for 15 days. The Pb concentrations in both Pb- and Pb + Zn-treated samples were significantly higher ($p < 0.01$) than that of the control group. The samples from Zn- and Pb + Zn-treated groups had significant amounts ($p < 0.01$) of Zn in the aboveground parts. Interestingly, the concentration of Zn in the Pb + Zn-treated group was significantly higher ($p < 0.05$) than that in Zn-treated group, which suggested synergism between Pb and Zn in *S. salsa*.

Table 3 Accumulated concentrations (μg g^{-1} dry weight) of lead and zinc in the aboveground parts of *S. salsa* after exposure to Pb, Zn, and their combination for 15 days

Treatment	Control	Pb	Zn	Pb + Zn
Pb	0.65 ± 0.15	1.19 ± 0.18**	0.63 ± 0.18	1.21 ± 0.22**
Zn	35.14 ± 3.32	36.86 ± 3.70	45.70 ± 4.03**	56.23 ± 4.87**

Values are presented as the mean ± SD ($n = 4$)

Significant difference (** $p < 0.01$) between control and heavy-metal-treated groups was tested by one-way analysis of variance

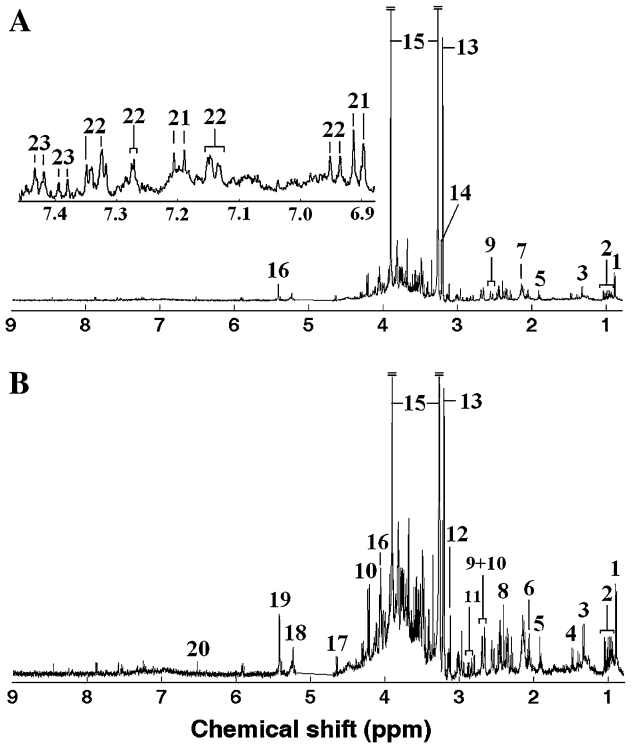

Fig. 2 A representative 1D 500 MHz ^{1}H-NMR spectrum of tissue extracts from the aboveground parts of *S. salsa* using the extraction solvent system of methanol/water (1/1) (**a**) and corresponding generalized log-transformed form (**b**). Metabolite assignments were based on certain chemical shift(s) of corresponding proton(s). *1* unknown 1 (0.88 ppm), *2* branched chain amino acids: leucine, isoleucine and valine, *3* threonine, *4* alanine, *5* acetate, *6* glutamate, *7* glutamine, *8* succinate, *9* malate, *10* aspartate, *11* asparagine, *12* malonate, *13* choline, *14* phosphocholine, *15* betaine, *16* fructose, *17* β-glucose, *18* α-glucose, *19* glycogen, *20* fumarate, *21* tyrosine, *22* ferulate, and *23* phenylalanine

Metabolic Responses

Figure 2 is a representative ^{1}H-NMR spectrum in original (Fig. 2a) and generalized log-transformed (Fig. 2b) forms of tissue extracts from the aboveground parts of *S. salsa* in the control group. Several classes of metabolites, including amino acids (valine, isoleucine, leucine, threonine, aspartate, tyrosine), osmolyte (betaine), carbohydrates (glucose and fructose), organic acids (succinate, fumarate, malate,

and ferulate), and phosphagen (phosphocholine), were identified and labeled (Fig. 2). Basically, the organic osmolyte betaine (3.25 and 3.91 ppm) was the most abundant metabolite in the aboveground parts of *S. salsa*.

Principal components analysis (PCA) was performed on the ^{1}H-NMR spectral data sets generated from control (red inverted triangles) and heavy-metal-exposed groups (green circles) of *S. salsa* after exposure for 15 days (Fig. 3). The control and Pb-treated groups were not significantly ($p > 0.05$) separated along any PC axis from the PC scores plot (data not shown). For the Zn and Pb + Zn exposures, PCA resulted in separations along the PC2 ($p = 0.067$) and PC3 ($p = 0.088$) axes, respectively, with statistical significance approaching 0.05 (Fig. 3a, b). To test the significance of metabolites between control and heavy-metal-exposed samples, one-way ANOVA was applied to find significant metabolic differences induced by heavy-metal exposures. In Pb-exposed *S. salsa* samples, only decreased tyrosine was observed, with statistical significance approaching 0.05. The significant metabolic differences, including increased branched-chain amino acids (valine, isoleucine, and leucine), threonine, alanine, asparagine, phenylalanine, and phosphocholine and decreased acetate, glycine, glucose, fumarate, and ferulate were detected in Zn-treated *S. salsa* samples (Table 4). The metabolic profile of the Pb + Zn-exposed group showed clear increases in branched-chain amino acids, alanine, asparagine, tyrosine, and phenylalanine and decreases in acetate, succinate, aspartate, malonate, fructose, glucose, fumarate, and ferulate (Table 4).

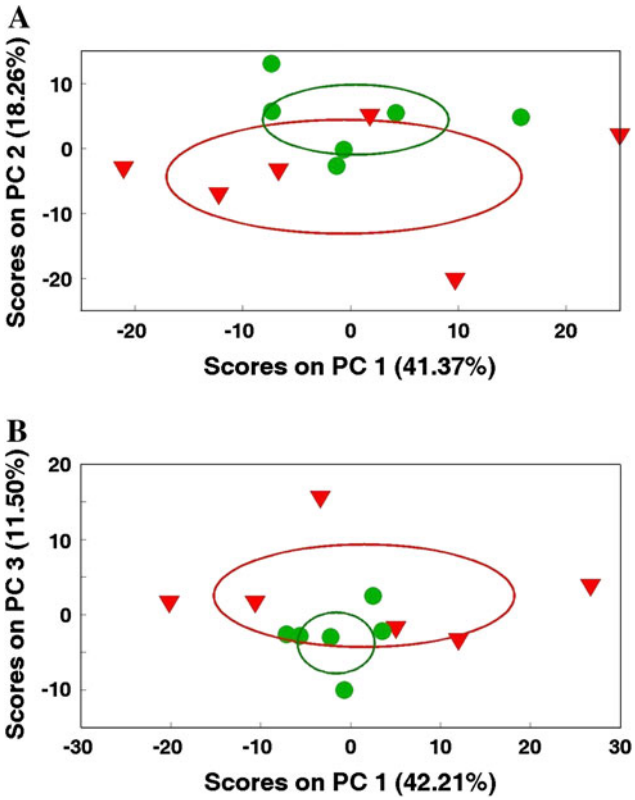

Fig. 3 PCA scores plots from the analysis of the 1D ^{1}H-NMR spectra of tissue extracts from the aboveground parts of *S. salsa* from control (*inverted triangle*) and heavy-metal-exposed (*circle*) groups, including 100 μg L^{-1} Zn (**a**) and mixed Pb (20 μg L^{-1}) and Zn (100 μg L^{-1}) (**b**) after exposure for 15 days. *Ellipses* represent mean ± SD of PC scores along PC axes for each group

Gene Expression Quantification

Our previous work reported that cadmium could induce both osmotic and oxidative stress in *S. salsa* (Liu and others 2011a). Here, the expression levels of three key osmotic regulation-involved genes (*INPS*, *CMO*, and *BADH*), two antioxidant enzyme genes (*CAT* and *GPx*), and one photosynthesis-related gene (*MDH*) were quantified using RT-PCR. After exposure to Pb, Zn, and mixed Pb and Zn for 15 days, the average expression levels of *CAT* genes were significantly ($p < 0.05$) upregulated in *S. salsa* samples (Fig. 4). For the osmotic regulation-involved genes, only *BADH* expression levels were downregulated in both single heavy-metal-exposed groups, with statistical significance approaching 0.05.

Discussion

After exposure for 15 days, *S. salsa* growth was significantly (ANOVA, $p < 0.05$) inhibited by exposure to Pb and Pb + Zn in terms of decreased weight or length. Although the average weight of *S. salsa* seedlings in the Zn-exposed group was not significantly lower than that of the control group, the statistical significance ($p = 0.055$) approached 0.05 (Table 2). Obviously, all three heavy-metal exposures inhibited plant growth after 15 days. As a known toxicant to organisms, lead can induce various types of toxicity, including genotoxicity, immunotoxicity, and nephrotoxicity, and can inhibit the growth of organisms (Zurich and others 2002; van Wijngaarden and Dosemeci 2006; Jain and others 2007). Conjecturally, lead should inhibit the growth of plants; this was observed in this work. Although Zn is essential to plants, excessive Zn induces adverse effects in both animals and plants (Yang and others 2011). In our case, the environmentally relevant level of Zn used (100 μg L^{-1}) inhibited the growth of *S. salsa* as well. This indicates that this concentration of Zn was harmful to *S. salsa* after exposure for 15 days. Interestingly, the length of *S. salsa* seedlings from the Pb + Zn-exposed group was lower than the lengths of both single heavy-metal-exposed samples. This implies the synergistic effects of Pb and Zn on *S. salsa*, which was observed in metal accumulation as well.

Table 4 Metabolite concentrations (μmol g^{-1} wet tissue) in the aboveground parts of *S. salsa* exposed to heavy metals

Metabolites[a]	Chemical shift (ppm, multiplicity)	Exposures			
		Control	Pb	Zn	Pb + Zn
Valine	1.05 (d)	0.37 ± 0.09	0.43 ± 0.06	0.51 ± 0.02**	0.51 ± 0.06**
Isoleucine	1.00 (d)	0.33 ± 0.08	0.37 ± 0.06	0.45 ± 0.03**	0.44 ± 0.03*
Leucine	0.94 (t)	0.31 ± 0.05	0.37 ± 0.06	0.40 ± 0.08*	0.39 ± 0.07*
Threonine	1.34 (d)	0.39 ± 0.08	0.43 ± 0.05	0.48 ± 0.05*	0.46 ± 0.06
Alanine	1.48 (d)	0.58 ± 0.06	0.61 ± 0.08	0.69 ± 0.12[#]	0.70 ± 0.13*
Acetate	1.91 (s)	0.05 ± 0.02	0.04 ± 0.01	0.03 ± 0.01*	0.03 ± 0.01**
Glutamate	2.05 (m)	3.85 ± 0.78	4.43 ± 0.53	4.45 ± 0.83	3.81 ± 0.61
Glutamine	2.14 (m)	2.15 ± 0.69	2.15 ± 0.77	2.84 ± 0.73	2.36 ± 0.64
Malate	2.68 (dd)	1.00 ± 0.57	1.82 ± 1.09	1.16 ± 0.37	0.56 ± 0.31
Succinate	2.41 (s)	0.50 ± 0.21	0.44 ± 0.13	0.41 ± 0.14	0.27 ± 0.13*
Aspartate	2.68 (ABX)	1.15 ± 0.18	1.13 ± 0.18	1.11 ± 0.21	0.90 ± 0.14*
Asparagine	2.85 (ABX)	1.14 ± 0.30	1.13 ± 0.32	1.78 ± 0.49*	1.70 ± 0.65[#]
Malonate	3.13 (s)	0.16 ± 0.02	0.17 ± 0.02	0.21 ± 0.06	0.22 ± 0.05*
Choline	3.19 (s)	1.58 ± 0.16	1.58 ± 0.09	1.55 ± 0.12	1.48 ± 0.05
Phosphocholine	3.21 (s)	0.34 ± 0.09	0.31 ± 0.07	0.42 ± 0.04	0.75 ± 0.88
Betaine	3.27 (s)	34.72 ± 3.47	34.97 ± 2.21	32.09 ± 1.29	34.89 ± 2.44
Glycine	3.57 (s)	0.20 ± 0.02	0.20 ± 0.02	0.15 ± 0.02**	0.18 ± 0.02
Fructose	4.01 (m)	0.91 ± 0.12	0.98 ± 0.18	0.70 ± 0.25	0.60 ± 0.09**
Glucose	4.64 (d), 5.23 (d)	2.88 ± 0.34	2.90 ± 0.27	1.94 ± 0.28**	1.81 ± 0.27**
Fumarate	6.52 (s)	0.10 ± 0.06	0.05 ± 0.02[#]	0.05 ± 0.03[#]	0.04 ± 0.02*
Tyrosine	6.91 (d)	0.16 ± 0.04	0.12 ± 0.02[#]	0.16 ± 0.03	0.19 ± 0.02[#]
Ferulate	7.32 (d)	0.11 ± 0.04	0.08 ± 0.02[#]	0.03 ± 0.01**	0.05 ± 0.01**
Phenylalanine	7.39 (m)	0.16 ± 0.03	0.19 ± 0.03	0.27 ± 0.05**	0.25 ± 0.03**

s singlet, *d* doublet, *dd* double doublet, *t* triplet, *m* multiplet, *ABX* complex multiplet involving 2 protons (A and B) and a heavy atom (X)

Values are presented as mean ± SD

[a] Statistical significances (* $p < 0.05$; ** $p < 0.01$) between control and heavy-metal-exposed *S. salsa* samples were determined by one-way ANOVA

[#] Statistical significance approached 0.05 ($p < 0.1$)

Both Zn and Pb + Zn exposures significantly ($p < 0.05$) increased the activities of antioxidant enzymes, including SOD, GPx, and CAT, in the aboveground parts of *S. salsa* seedlings (Fig. 1). The significantly ($p < 0.05$) upregulated activities of POD were observed only in Zn-exposed *S. salsa* samples. In Pb-exposed *S. salsa* samples, only CAT activities were significantly ($p < 0.05$) upregulated. However, there were no significant alterations to GST activities in any heavy-metal-exposed *S. salsa* groups. Because most heavy-metal contaminants can produce reactive oxygen species (ROS) which damage biological molecules such as DNA and lipids (Rainbow 1995; Ekmekci and others 2009), these findings confirmed the oxidative stress induced by both Zn and mixed Pb and Zn in *S. salsa*. Pb exposure seemed to induce only slight oxidative stress because only CAT activity was increased in the aboveground parts of *S. salsa* (Dinakar and others 2012; Kadioglu and others 2012). In Pb + Zn-treated samples, therefore, Zn induced the oxidative stress rather than Pb. At the gene expression level, only *CAT* gene expression levels were significantly upregulated in all heavy-metal-exposed *S. salsa* samples, which was consistent with the upregulation of CAT activities.

There was no significant separation between control and Pb-treated groups after exposure for 15 days (data not shown). Moreover, no significant metabolic changes were found in the Pb-exposed samples except decreased tyrosine, with a statistical significance approaching 0.05. This clearly demonstrates that Pb did not induce severe toxicities at the metabolic level during the 15 days of exposure. Amino acids, including valine, leucine, isoleucine, threonine, alanine, asparagine, and phenylalanine, were significantly increased in the aboveground parts of *S. salsa* seedlings with Zn exposure. Interestingly, the total protein content in the aboveground parts of *S. salsa* seedlings after Zn exposure was highly significantly ($p < 0.01$) decreased (data not shown). This means that upregulated protein biodegradation in *S. salsa* was caused by Zn exposure. The

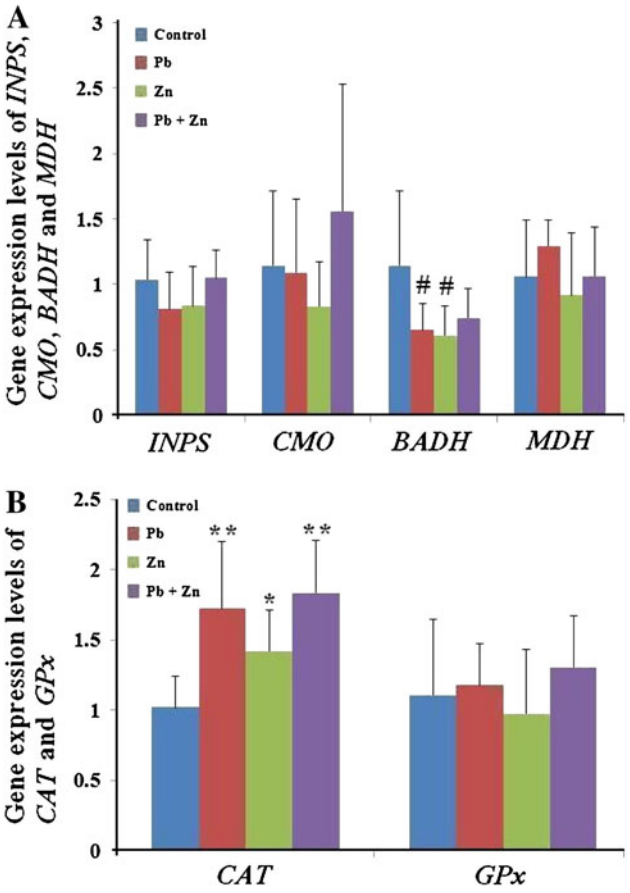

Fig. 4 Expression levels of osmotic-related (*INPS*, *CMO*, and *BADH*) and photosynthesis-related (*MDH*) enzyme genes (**a**) and *CAT* and *GPx* antioxidant enzyme genes (**b**) in the aboveground parts of seedlings of *S. salsa* from control, Pb, Zn, and mixed Pb and Zn-treated groups after exposure for 15 days. Data ($n = 6$) were expressed as mean ± SD. Significant difference among groups was tested by one-way analysis of variance with Tukey's test and indicated by * ($p < 0.05$). # Statistical significance between control and exposed groups approached 0.05 ($p < 0.1$)

carbohydrate glucose was significantly decreased in Zn-exposed *S. salsa* samples. In plant cells, carbohydrates (sugars) such as glucose, fructose, and sucrose are commonly derived from photosynthesis and gluconeogenesis. Thus, decreased glucose might imply that photosynthesis and/or gluconeogenesis were/was inhibited by Zn exposure in *S. salsa*. Fumarate is a key intermediate in the tricarboxylic acid (TCA) cycle. The decrease in fumarate indicated disturbances in the TCA cycle that were related to energy metabolism induced by Zn exposure in *S. salsa*. Ferulate is one of the phenolic acids in plants that occur in seeds and leaves. It also has antioxidant potential to reactive oxygen species due to its phenolic nucleus. As mentioned above, Zn could induce oxidative stress in *S. salsa*; therefore, the significant decrease in ferulate in Zn-treated *S. salsa* samples could be accounted for by its antioxidant potential to protect the plant from ROS damage (Remans and others 2012).

Besides the similar metabolic responses of amino acids, some unique metabolic biomarkers, including increased succinate, aspartate, and malonate and decreased fructose, were found in the aboveground parts of *S. salsa* exposed to Pb + Zn. Succinate is another key intermediate in the TCA cycle, which implied disturbance in energy metabolism. As discussed above, decreased fructose could also imply that photosynthesis and/or gluconeogenesis were/was inhibited by combined Pb and Zn exposure in *S. salsa*. All these differential metabolic responses in Pb + Zn-exposed *S. salsa* samples indicate that Pb and Zn induce synergistic effects.

In conclusion, the regulation of metabolites, gene expression, and antioxidant enzymes was characterized in *S. salsa* exposed to environmentally relevant lead and zinc. The significant metabolic biomarkers included amino acids (valine, isoleucine, leucine, threonine, asparagine, and phenylalanine) and decreased acetate, glucose, ferulate, and fumarate in *S. salsa* exposed to Zn for 15 days. The increased succinate, aspartate, and malonate and decreased fructose were found only in mixed Pb + Zn-exposed samples in addition to the similar metabolic changes such as alanine, glucose, fumarate, and ferulate in Zn-exposed samples. Both Zn and mixed Pb and Zn exposures significantly ($p < 0.05$) upregulated the activities of antioxidant enzymes, including SOD, GPx, and CAT in the aboveground parts of seedlings. However, only *CAT* (AW990998) gene expression levels were significantly ($p < 0.05$) elevated in *S. salsa* exposed to all the heavy-metal groups. Based on the metabolic biomarkers, gene expressions, and antioxidant enzyme activities, both Zn and mixed Pb and Zn induced significant oxidative disturbances in photosynthesis/glucogenesis, energy metabolism, and protein biodegradation in *S. salsa*. However, the environmentally relevant Pb could induce slight oxidative stress in *S. salsa* indicated by upregulated catalase gene expression levels and CAT activities.

Acknowledgments We thank Dr. Mark Viant (School of Bioscience, The University of Birmingham) for use of the software Pro-Metab. This research was supported by the Project of National Science and Technology Pillar Program in the "12th Five Year" Period (2011BAC02B01) and The 100 Talents Program of the Chinese Academy of Sciences.

References

Bradford M (1976) A rapid and sensitive method for the quantification of microgram quantities of protein utilizing the principle of protein–dye binding. Anal Biochem 72:248–254

Dinakar C, Djilianov D, Bartels D (2012) Photosynthesis in desiccation tolerant plants: energy metabolism and antioxidative stress defense. Plant Sci 182:29–41

Ekmekci Y, Tanyolac D, Ayhan B (2009) A crop tolerating oxidative stress induced by excess lead: maize. Acta Physiol Plant 31:319–330

Fan WMT (1996) Metabolite profiling by one- and two-dimensional NMR analysis of complex mixtures. Prog Nucl Magn Reson Spectrosc 28:161–219

Garg N, Aggarwal N (2011) Effects of interactions between cadmium and lead on growth, nitrogen fixation, phytochelatin, and glutathione production in mycorrhizal *Cajanus cajan* (L.) millsp. J Plant Growth Regul 30:286–300

Greenway H, Osmond CB (1972) Salt responses of enzymes from species differing in salt tolerance. Plant Physiol 49:256–259

Han N, Shao Q, Lu CM, Wang BS (2005) The leaf tonoplast V-H^+-ATPase activity of a C3 halophyte *Suaeda salsa* is enhanced by salt stress in a Ca-dependent mode. J Plant Physiol 162:267–274

Hines A, Yeung WH, Craft J, Brown M, Kennedy J, Bignell J, Stentiford GD, Viant MR (2007) Comparison of histological, genetic, metabolomics, and lipid-based methods for sex determination in marine mussels. Anal Biochem 369:175–186

Hogstrand C, Wood CM (1996) The physiology and toxicology of zinc in fish. In: Taylor EW (ed) Toxicology of aquatic pollution: physiological, cellular and molecular approaches, society for experimental biology, seminar series: 57. Cambridge University Press, Cambridge, pp 61–84

Hoshino E, Frölander F, Carlsson J (1978) Oxygen and the metabolism of *Peptostreptococcus anaerobius* VPI4330-1. J Gen Microbiol 107:235–238

Jain NB, Potula V, Schwartz J, Vokonas PS, Sparrow D, Wright RO, Nie H, Hu H (2007) Lead levels and ischemic heart disease in a prospective study of middle-aged and elderly men: the VA Normative Aging Study. Environ Health Perspect 115:871–875

Kadioglu A, Terzi R, Saruhan N, Saglam A (2012) Current advances in the investigation of leaf rolling caused by biotic and abiotic stress factors. Plant Sci 182:42–48

Keun HC, Ebbels TMD, Antti H, Bollard ME, Beckonert O, Holmes E, Lindon JC, Nicholson JK (2003) Improved analysis of multivariate data by variable stability scaling: application to NMR-based metabolic profiling. Anal Chim Acta 490:265–276

Kim HK, Verpoorte R (2010) Sample preparation for plant metabolomics. Phytochem Anal 21:4–13

Li PH, Chen M, Wang BS (2002) Effect of K^+ nutrition on growth and activity of leaf tonoplast V-H^+-ATPase and V-H^+-PPase of *Suaeda salsa* under NaCl stress. Acta Bot Sin 44:433–440

Li PH, Wang ZL, Zhang H, Wang BS (2004) Cloning and expression analysis of the B subunit of V-H^+-ATPase in the leaves of *Suaeda salsa* under NaCl stress. Acta Bot Sin 46:93–99

Li X, Xiang XM, Zhou JT, Qu BC, Zhou XB (2007) Advance of study on soil remediation and sewage treatment by halophyte *Suaede salsa*. Jiangsu Environ Sci Technol 20:53–54 (in Chinese)

Li L, Liu X, Peijnenburg WJGM, Zhao J, Chen X, Yu J, Wu H (2012) Pathways of cadmium fluxes in the root of the halophyte *Suaeda salsa*. Ecotoxicol Environ Saf 75:1–7

Liu X, Yang C, Zhang L, Li L, Liu S, Yu J, You L, Zhou D, Xia C, Zhao J, Wu H (2011a) Metabolic profiling of cadmium-induced effects in one pioneer intertidal halophyte *Suaeda salsa* by NMR-based metabolomics. Ecotoxicology 20:1422–1431

Liu X, Zhang L, You L, Wu H, Zhao J, Cong M, Li F, Wang Q, Li L, Li C, Han G, Wang G, Xia C, Yu J (2011b) Metabolomic study on the halophyte *Suaeda salsa* in the Yellow River Delta. Clean Soil Air Water 39:720–727

Livak KJ, Schmittgen TD (2001) Analysis of relative gene expression data using real-time quantitative PCR and the 2(-Delta Delta C(T)) method. Methods 25:402–408

Mao TY, Dai MX, Peng ST, Li GL (2009) Temporal-spatial variation trend analysis of heavy metals (Cu, Zn, Pb, Cd, Hg) in Bohai Bay in 10 years. J Tianjin Univ 9:817–825 (in Chinese)

Nelson DE, Rammesmayer G, Bohnert HJ (1998) Regulation of cell-specific insitol metabolism and transport in plant salt tolerance. Plant Cell 10:753–764

Noriega G, Cruz DS, Batlle A, Tomaro M, Balestrasse K (2012) Heme oxygenase is involved in the protection exerted by jasmonic acid against cadmium stress in soybean roots. J Plant Growth Regul 31:79–89

Parsons HM, Ludwig C, Gunther UL, Viant MR (2007) Improved classification accuracy in 1- and 2-dimensional NMR metabolomics data using the variance stabilising generalised logarithm transformation. BMC Bioinformatics 8:234

Rainbow PS (1995) Biomonitoring of heavy metal availability in marine environment. Mar Pollut Bull 31:183–192

Remans T, Opdenakker K, Guisez Y, Carleer R, Schat H, Vangronsveld J, Cuypers A (2012) Exposure of *Arabidopsis thaliana* to excess Zn reveals a Zn-specific oxidative stress signature. Environ Exp Bot 84:61–71

Sun R, Zhou Q, Wei S (2011) Cadmium accumulation in relation to organic acids and nonprotein thiols in leaves of the recently found Cd hyperaccumulator *Rorippa globosa* and the Cd-accumulating plant *Rorippa islandica*. J Plant Growth Regul 30:83–91

van Wijngaarden E, Dosemeci M (2006) Brain cancer mortality and potential occupational exposure to lead: findings from the national longitudinal mortality study, 1979–1989. Int J Cancer 119:1136–1144

Vernon DM, Bohnert HJ (1992) A novel methyl transferase induced by osmotic stress in the facultative halophyte *Mesembryanthemum crystallinum*. EMBO J 11:2077–2086

Wang BS, Luttge U, Ratajczak R (2001) Effects of salt treatment and osmotic stress on V-ATPase and V-PPase in leaves of the halophyte *Suaeda salsa*. J Exp Bot 52:2355–2365

Wang BS, Luttge U, Ratajczak R (2004) Specific regulation of SOD isoforms by NaCl and osmotic stress in leaves of C3 halophyte. J Plant Physiol 161:285–293

Wu H, Liu X, You L, Zhang L, Zhou D, Feng J, Zhao J, Yu J (2012) Effects of salinity on metabolic profiles, gene expressions and antioxidant enzymes in halophyte *Suaeda salsa*. J Plant Growth Regul. doi:10.1007/s00344-011-9244-6

Xu L (2004) Methods of chemometrics. Science Press, Beijing, pp 221–227

Xu CY, Liu XB, Liu ZG, Wang J, Jiang ZP, Cao JL (2007) Remedial effect of *Suaeda salsa* Pall planting on the oil polluted coastal zones. J Saf Environ 1:37–39

Yang Y, Sun C, Yao Y, Zhang Y, Achal V (2011) Growth and physiological responses of grape (*Vitis vinifera* "Combier") to excess zinc. Acta Physiol Plant 33:1483–1491

Zhang X (2001) Investigation of pollution of Pb, Cd, Hg, As in sea water and deposit of Bohai Sea area. Heilongjiang Environ J 25:87–90 (in Chinese)

Zhang L, Ma XL, Zhang Q, Ma CL, Wang PP, Sun YF, Zhao YX, Zhang H (2001) Expressed sequence tags from a NaCl-treated *Suaeda salsa* cDNA library. Gene 267:193–200

Zhao KF (1991) Desalinization of saline soils by *Suaeda salsa*. Plant Soil 135:303–305

Zhou MJ, Yan T (1997) Progress in marine ecotoxicology study in China. Res Mar Environ 3:1–5 (in Chinese)

Zhu MH, Ding YS, Zheng DC, Tao P, Ji YX, Cui Y, Gong WM, Ding DW (2005) Accumulation and tolerance of Cu, Zn, Pb and Cd in plant *Suaeda heteroptera Kitag* in tideland. Mar Environ Sci 24:13–16

Zurich G, Eskes C, Honegger P (2002) Maturation-dependent neurotoxicity of lead acetate in vitro: implication of glial reactions. J Neurosci Res 70:108–116